# Comparison of MM-ALE and SPH methods for modelling blast wave reflections of flat and shaped surfaces

Jovan Trajkovski

University of Ljubljana, Faculty of Mechanical Engineering, Chair of Modelling in Engineering Science and Medicine

## Abstract

The Multi-Material Arbitrary-Language-Euler (MM-ALE) and Smooth-Particle-Hydrodynamics (SPH) are widely used methods for numerical examination of the structural response under blast loading. On the other hand, the methods are quite demanding for use. They have their own advantages and disadvantages depending on the structural geometry and its relative position with regard to the blast wave source location. This paper presents comparison results of a detailed numerical examination using both the MM-ALE and SPH method. A series of simulation tests were performed using flat and shaped armour steel plates in LS-DYNA. The comparison results showed that the SPH method offers better results and efficiency compared to the MM-ALE method. This is especially evident in cases involving curved structural geometry. The results of this paper are important in the decision making process when choosing an appropriate method for blast response analyses of structures.

Keywords: blast wave; SPH; MM-ALE; blast loading; blast response

## 1 Introduction

Blast response examination is of great importance when designing safe and effective military as well as civilian equipment or structures. Preparation and performance of experiments involving high explosives is extremely expensive and time consuming even for small scale tests in laboratory conditions, analytical results are not even possible for complex structural geometries, which makes numerical analysis a valuable tool for examination. Therefore, it is necessary to have a simple and reliable numerical modelling technique in order to successfully design structures exposed to this high-intensity, short-duration loads.

The most popular numerical techniques for modelling blast response of structures currently available in LS-DYNA are:

- **ConWep (*LOAD_BLAST_ENHANCED)** used generally for applying uniform loading to structures at a distance about three times greater than the charge radius [1, 2]. The method ignores blast wave reflections and blast wave interactions of multiple explosions.
- **MM-ALE (Multi Material Arbitrary Lagrange Euler) (S-ALE).** The method allows explosives and air to be represented as separated materials with a possibility to shear the same elements in the model ([3, 4]). All the processes, starting with the detonation, blast wave formation and its interaction with the surrounding structures through Fluid Structure Interaction (FSI) algorithm can be modelled. This enables more precise presentation of blast wave formation allowing more complicated scenarios to be analysed. It is generally recommended for close range explosions but it is also used at higher scaled distances if combined with other techniques such as coupling with the empirical *LOAD_BLAST_ENHANCED [5] or the ALE

mapping technique [6, 7]. The MM-ALE method was successfully used in the past in different loading scenarios [7-20].

- **SPH (Smooth Particle Hydrodynamics).** The SPH method has proved to be a reliable and efficient method for modelling the blast response of military vehicles and other structures [21-27], although it is not recommended for use in blast response analyses. It is a time-efficient method which does not require the surrounding air to be represented in the model because it is difficult to track the blast wave loading parameters at a certain point in the space [21].
- **CPM (Corpuscular Particle Method) PARTICLE_BLAST**. The corpuscular approach proposed by [28] and successfully applied by [29] is based on the Kinetic Molecular Theory (KMT) which represents the study of gas molecules and their interactions [30]. The CPM modelling technique was not considered in this study, even though it is a promising and relatively new modelling technique [31].

Although some general recommendations can be found in the literature for each of the modelling techniques, no recommendations are available for the selection of the most appropriate one. The aim of this study is to compare the structural response results of blast loaded flat and V-shape plates using the MM-ALE and SPH modelling techniques and recommend the most appropriate modelling technique based on the results obtained.

## 2 Experiments and numerical models description

The experiments described in this session (Table 1) are based on the part of the work by Neuberger et al. [32]. A 10 mm rolled homogenous armour (RHA) circular plates of diameter 0.5 m were exposed to free air bursts of TNT charges of $m_{TNT}$ = 0.468 kg and $m_{TNT}$ = 1.094 kg at close range stand-off distances of $h_{SoD}$ = 0.1 m and $h_{SoD}$= 0.065 m. The corresponding scaled distances varied between $Z$ = 0.063 m/kg$^{1/3}$ and $Z$ = 0.128 m/kg$^{1/3}$ (Table 1).

| $D$ (m) | $t$ (mm) | $m_{TNT}$ (kg) | $h_{SoD}$ (m) | $Z$ (m/kg$^{1/3}$) |
|---|---|---|---|---|
| 0.5 | 10 | 0.468 | 0.1 | 0.063 |
| 0.5 | 10 | 1.094 | 0.1 | 0.097 |
| 0.5 | 10 | 1.094 | 0.065 | 0.128 |

*Table 1: Tests by Neuberger et al. [32].*

Fig. 1 presents the MM-ALE and SPH model.

In both MM-ALE and SPH numerical models, one-fourth symmetry was used. The plates in both series of models were presented with four solid elements (Fig. 1) through thickness, using fully integrated accurate element formulation and a poor aspect ratio (ELFORM = -2). Instead of simply meshing the circular plate, it was represented as a square plate constraining the displacement in all directions of the nodes outside the circle with radius $R$ = 0.25 m, thus representing the circular camped plate.

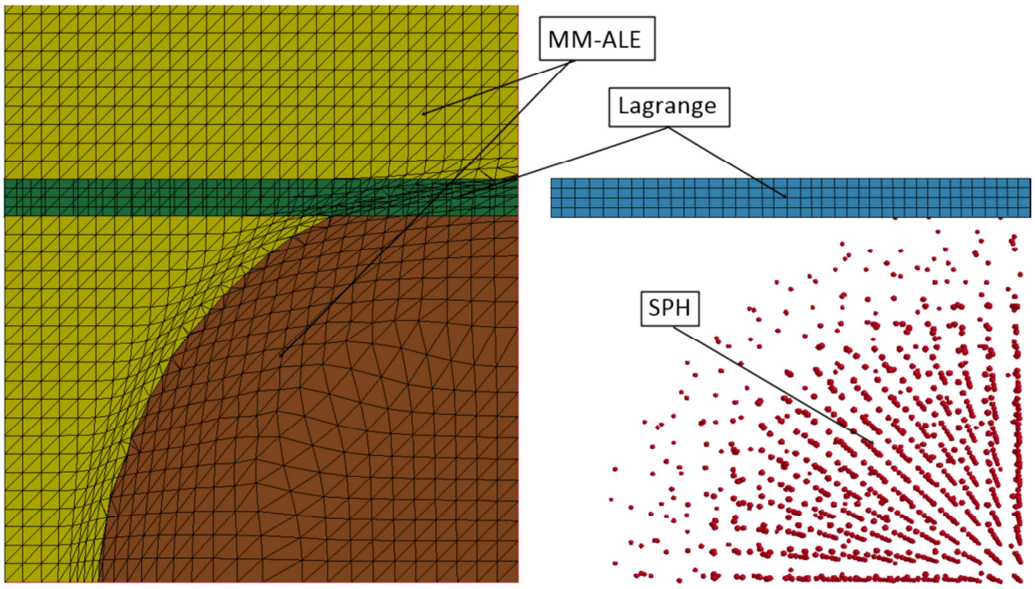


*Fig. 1: MM-ALE and SPH models*

### 2.1 MM-ALE models

In order to study the influence of the numerical parameters of the MM-ALE model, a series of numerical analyses were performed with boundary conditions placed at a different distances of the plate, various mesh sizes, advection methods (METH), mesh remapping factors (EFAC), time-step coefficients (TSSFAC), and relative size of the structural and fluid mesh (Table 2).

| *MM-ALE Model variants* | *1* | 2 | 3 | 4 | 5 | 6 |
|---|---|---|---|---|---|---|
| $h_{DoB}$ (m) | 0.5 | 0.4 | 0.35 | 0.30 | 0.25 | 0.20 |
| ALE mesh size (mm) | 50 | 25 | 12.5 | 6.25 | | |
| METH | 3 | -2 | | | | |
| EFAC | 1.000 | 0.100 | 0.050 | 0.01 | 0.005 | |
| TSSFAC | 0.4 | 0.6 | 0.8 | | | |
| nL vs nE | 4L vs 1E | 2L vs 1E | 1L vs 1E | 1L vs 2E | | |

*Table 2: MM-ALE models scheme presentation*

In the first step, a proper minimal distance of the boundary conditions of the plate structure was determined using mesh boxes of different sizes and equal element size as presented in [33]. After the selection of the distance of boundary conditions, simulations were performed with different mesh sizes in order to study the convergence of the solution and the mesh size influence on the results. In each of these models, the plate was represented with nearly two Lagrangian elements per one Eulerian, METH = 3, EFAC = 0.01 and TSSFAC = 0.6. Having defined the distance of the boundary conditions and mesh size, the study continued investigating the influence of selected advection method (METH), mesh remapping factor (EFAC), time-step coefficient (TSSFAC), and relative size of the structural and fluid mesh on the results. Although mesh biasing is generally recommended [33] as it can reduce the

size of the model improving the results, it also reduces the time step increasing the computational time. For that reason, only uniform mesh without biasing was used in all the models of this study. The fluids in this model are represented with 1 point multy-material-ALE element formulation (ELFORM = 11). This element formulation allows the explosive and air to be represented as separate materials with the possibility to shear the same elements in the model [3, 4]. The contact between the ALE fluids and steel plate was modelled using the well-known *CONSTRAINED_LAGRANGE_IN_SOLID card.

```
*CONSTRAINED_LAGRANGE_IN_SOLID_TITLE
$#  coupid                                                          title
         1
$#   slave    master     sstyp     mstyp     nquad     ctype     direc     mcoup
         1         1         2         0         3         4         1         0
$#   start       end      pfac      fric    frcmin      norm   normtyp      damp
     0.000   1.00E10      0.10     0.000      0.50         0         0     0.000
$#      cq      hmin      hmax     ileak     pleak   lcidpor     nvent  blockage
     0.000     0.000     0.000         0     0.010         0         0         0
$#  iboxid   ipenchk   intforc   ialesof    lagmul    pfacmm      thkf
         0         0         1         0     0.000         0     0.000
```

The spherical charge in the model was represented with the *INITIAL_VOLUME_FRACTION_GEOMETRY card defining the initial radius of the spherical charge. Readers interested in more details about the blast wave loading parameters validation procedures using MM-ALE modeling technique are reffered to the work of Trajkovski [33] and Schwer [34].

### 2.2 SPH model

For the purpose of studying the most influential numerical parameters of the SPH model, a series of numerical analyses were performed with different plate mesh sizes and a different number of SPH particles, various time-step coefficients (TSSFAC), smooth lengths coefficients (CSLH), contact forces coefficients (SOFSCL) of the soft constraint formulation (Table 3).

| *SPH Model variants* | *1* | 2 | 3 | 4 | 5 |
|---|---|---|---|---|---|
| No. of elements along plate radii vs charge radii | 20 Lag. (12.5 mm) vs 13 SPH | 40 L (6.25mm) vs 25 SPH | 80 L (3.125mm) vs 50 SPH | | |
| TSSFAC | 0.7 | 0.5 | 0.3 | 0.1 | 0.05 |
| SCLH | 1.3 | 1.1 | 1.0 | 0.9 | 0.8 |
| SOFSCL | 0.10 | 0.15 | 0.25 | 0.35 | |

*Table 3: SPH models scheme presentation*

To analyse the model mesh convergence in the first step, three numerical models with different mesh sizes or a different number of SPH particles were created. In the numerical model with the coarsest mesh, half side of the plate was modelled with 20 Lagrange elements and the TNT charge with 13 particles per radius. In the medium mesh model, the plate was modelled with 40 elements and the TNT charge with 25 particles per charge radius, whereas in the finest mesh model the plate was modelled with 80 elements and the TNT charge with 50 particles per radius.

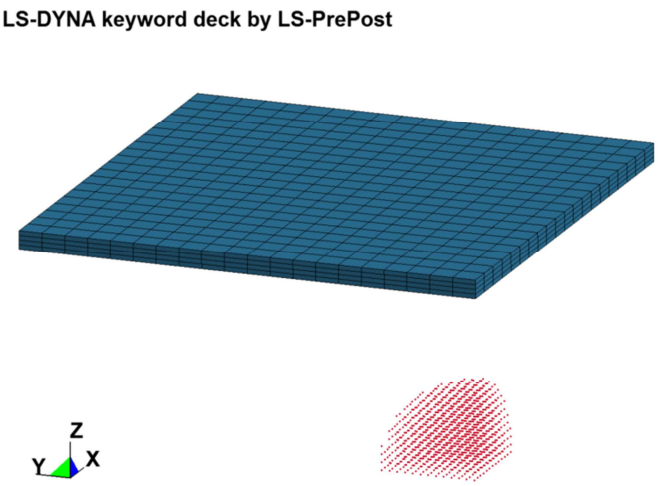


*Fig. 2 : Coarsest mesh of the SPH-model ()*

In the SPH model presented in Fig. 2 : the plate was modelled with 8-node fully integrated 3D elements (ELFORM -2), while the charge was modelled using SPH elements. The selected contact (CONTACT_AUTOMATIC_NODES_TO_SURFACES) between smoothed SPH particles and the plate is based on the penetration depth of individual nodes of a material (in this case discrete SPH particles) through the Lagrange plate. Based on their depth size in a given time step, the algorithm applies proportional forces with the aim of preventing their penetration (Constraint based contact). In the analysis with the SPH model, for better results comparison with the MMALE model all data on the plate geometry and material parameters were collected from Neuberger [32]

## 2.3 Material models

### *2.3.1 Explosive charge*

The explosive charge in both MM-ALE and SPH models was presented with *MAT_HIGH_EXPLOSIVE_BURN in combination with the Jones-Wilkins-Lee (JWL) equation of state (EOS)

$$p = A\left(1-\frac{\omega}{R_1 v}\right)exp^{-R_1 v} + B\left(1-\frac{\omega}{R_2 v}\right)exp^{-R_2 v} + \frac{\omega E}{v}, \quad (1)$$

which calculates blast pressure as a function of relative volume $v=\rho_0/\rho$ and internal energy $E$, for an explosive element. In this equation, $A$, $B$, $R_1$, $R_2$, and $\omega$ are parameters related to the explosive material and can be found in most of the explosive textbooks. They were taken from reference [35] for TNT high explosive and are given in Table 1.

| $\rho$(kg/m$^3$) | $D$(m/s) | $P_{CJ}$(GPa) | $A$(GPa) | $B$(GPa) | $R_1$(-) | $R_2$(-) | $\omega$(-) | $E$(J/m$^3$) |
|---|---|---|---|---|---|---|---|---|
| 1590 | 6930 | 21.0 | 3.712 | 3.231 | 4.15 | 0.95 | 0.3 | 7*10$^9$ |

*Table 4: Material properties and JWL parameters for TNT [35]*

*2.3.2 Air*

The air in the MM-ALE models was approximated as an ideal gas for which *MAT_NULL was used in combination with linear polynomial equation of state

$$p = (\gamma - 1)\frac{\rho}{\rho_0}E, \tag{2}$$

in which $\gamma$=1.4 is the ratio of the specific heats, $\rho$ is current density, $\rho_0 = 1.29$ kg/m$^3$ is initial density and E = 250 kJ represents initial internal energy of the air at atmospheric pressure of 1 bar.

| $\rho$ (kg/m$^3$) | $\gamma$ | $C_0$ | $C_1$-$C_3$, $C_6$ | $C_4$,$C_5$ | $E_0$ ( J ) | $V_0$ (/) |
|---|---|---|---|---|---|---|
| 1.29 | 1.4 | -1x10$^{-6}$ | 0 | 0.4 | 2.5x10$^5$ | 1 |

*Table 5: Material properties and linear polynomial EOS parameters for air*

*2.3.3 Steel*

Structural plate geometry (diameter D = 0.5 m, plate thickness t = 10 mm) in all the models was represented with a bilinear material model ( *MAT_PLASTIC_KINEMATIC ) and parameters representing the RHA steel were taken from [32].

| $\rho$ (kg/m$^3$) | $\nu$ | $\sigma_y$ ( MPa ) | $E$ ( GPa ) | $E_t$ ( GPa ) |
|---|---|---|---|---|
| 7850 | 0.3 | 1000 | 210 | 2 |

*Table 6: Material properties for RHA steel [32]*

## 3 Numerical parameters influence

### 3.1 MM-ALE

Fig. 3 presents the time-displacement results of the MM-ALE simulations. Fig. 3a presents the results for the models with boundary conditions placed at different distances from the plate. Time-displacement curves change until the 0.4 m box size, while no difference is visible with them further moving away (See Fig. 3a). In Fig. 3b, the influence of mesh size on structural displacement of the plate is presented. It is visible in Fig. 3b that the solution converges for the mesh size smaller than 12.5 mm. The results for two different advection methods are presented in Fig. 3c and no significant difference was observed between them, except that the total energy was preserved using the donor cell method (METH = 3). The results for the remapping factor for mesh smoothing in front of the blast wave (EFAC) are presented in Fig. 3d. The time-displacement curve of the plate converged for lower values than EFAC=0.01. It should also be noted that smaller EFAC values greatly reduce the computational time and can also lead to solution termination. Even the default time step in LS-DYNA is automatically decreased to a value of 0.67 if high explosives are used [2]. However, no considerable influence of the time step coefficient was observed in this study (Fig. 3e). The results for relative size of the Lagrangian vs Eulerian mesh are presented in Fig. 3f. It is evident that the converged solution

can be achieved for the Lagrange mesh 1 to 2 times smaller than the Eulerian mesh. Further refining of the Eulerian mesh can also lead to leakage problems causing loss of energy and unconverged solution (Fig. 3f, curve 4L vs 1E).

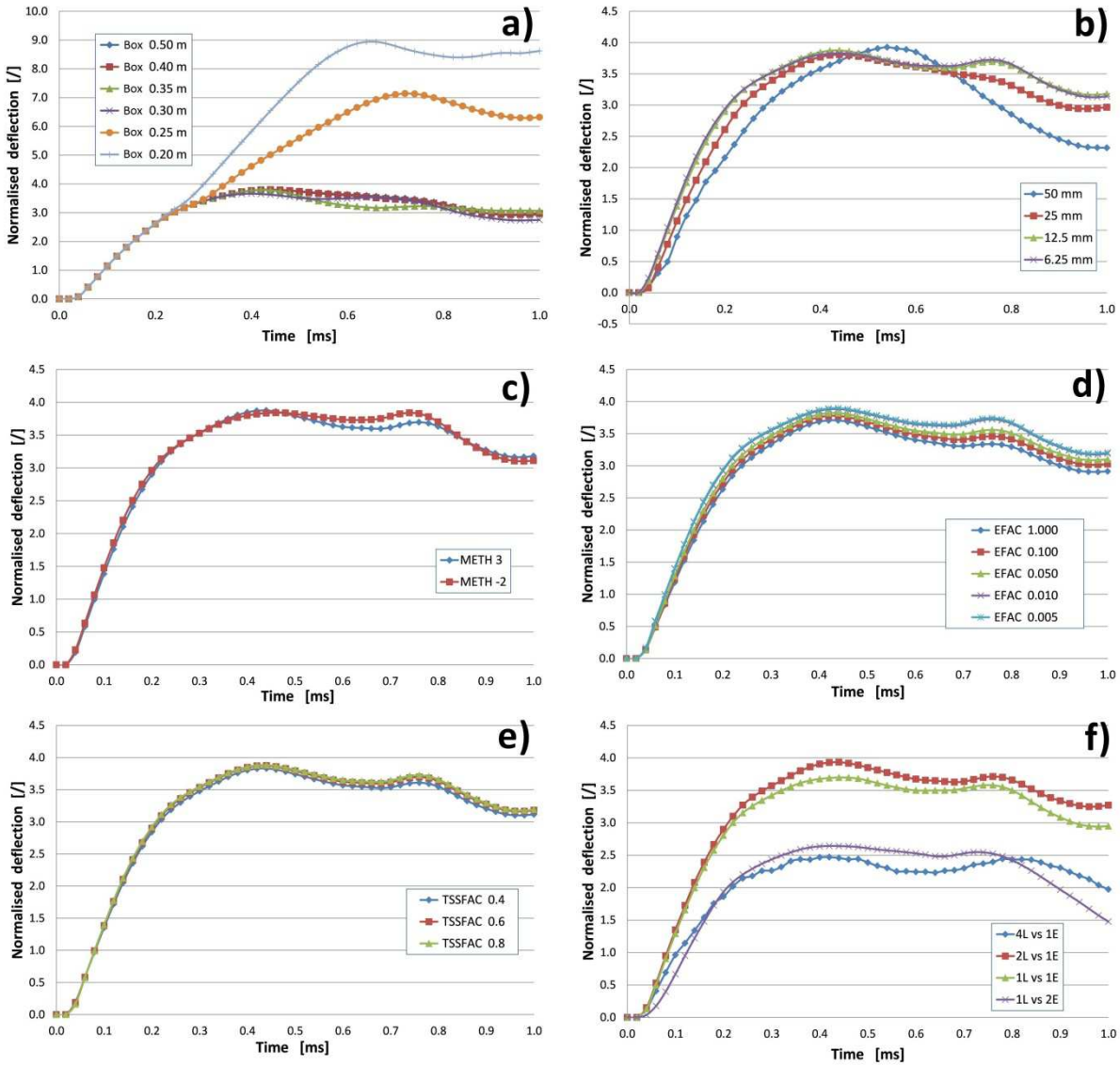


*Fig. 3: MM-ALE model: a) Distance of the boundary conditions, b) mesh size, c) Advection method (METH), d) Mesh remapping coef. (EFAC), f) Time step coef. (TSSFAC), f) Relative size of the structural and fluid mesh.*

Table 7 presents the summarised numerical parameters that lead to a converged solution in the given case.

| *MM-ALE Model variant* | Mesh box size | Mesh size | METH | EFAC | TSSFAC | NL vs nE |
|---|---|---|---|---|---|---|
| *Converged solution value* | 0.4 m | 12.5 mm | 3 | 0.01 | 0.8 | 2L vs 1E |

*Table 7: Selection of the appropriate MM-ALE model parameters*

### 3.2 SPH

Fig. 3 presents the time-displacement results of the SPH model simulations. As shown in Fig. 4a, the value of the normalized displacement converges as the mesh is refined. However, there is no significant difference in the plate response between the medium mesh model and finest mesh model. It should also be noted that computational time is extended from 6 minutes for the medium mesh model to 34 minutes for the model with the finest mesh.

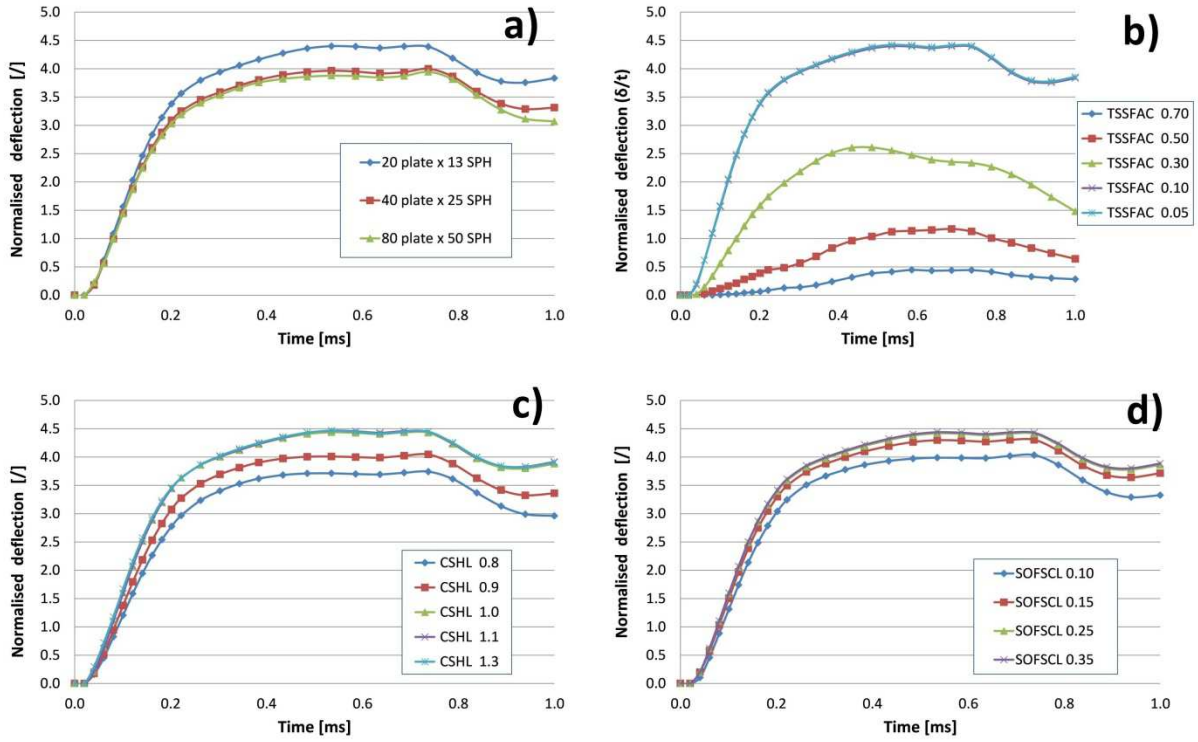


*Fig. 4: SPH-model results: a) Mesh size, b) Time step coef. (TSSFAC), c) Smooth length coef. (CSHL) and d) Contact forces coef. (SOFSCL)*

Besides the impact of the mesh size, the time step also has a significant influence on the SPH model results. By decreasing the time step coefficient (TSSFAC) and using the appropriate combination of contact parameters, transmission of kinetic energy from the TNT charge to the plate is significantly improved. Consequently, the normalized time-displacement curve converges at a specific value of the time step coefficient, which in this case equals to 0.1 (Fig. 4b).

LS-DYNA controls the size of the smoothing length by means of the CSHL coefficient the default value of which is 1.2. The initial smoothing length is calculated as the maximum value of all the minimum distances for each SPH particle. As evident in Fig. 4c, the default value (CSHL) corresponds to the converged value of the plate response, which coincides with the instructions given in the manual [2].

Since the soft constrained formulation option was activated (SOFT=1), the value of the constraint forces can be controlled by means of the SOFSCL coefficient. As evident in Fig. 4c, the satisfactory converged value of the SOFSCL coefficient is 0.25. Table 8 presents the summarised numerical parameters that lead to a converged solution in the given case.

| *SPH Model variant* | No. of elements along plate radii vs charge radii | TSSFAC | SCLH | SOFSCL |
|---|---|---|---|---|
| *Converged solution value* | 40 L (6.25mm) vs 25 SPH | 0.1 | 1.1 | 0.25 |

*Table 8: Selection of the appropriate SPH model parameters*

## 4 Results comparisons (MM-ALE vs. SPH)

### 4.1 Flat plate

The converged numerical parameters of both models presented in Section 3 were determined based on the case ($m_{TNT}$ = 1.094 kg, $h_{SoD}$ = 0.1 m) by Neuberger et. Al. [32] and applied to the other two loading cases ($m_{TNT}$ = 1.094 kg, $h_{SoD}$ = 0.065 m and $m_{TNT}$ = 0.468 kg, $h_{SoD}$ = 0.1 m). Fig. 5 presents the time-displacement histories of both models for all three loading cases. The experimental maximum plate displacements for the loading cases are also presented in the same figure. Despite the fact that both models generally underestimate the experimental results, the SPH–model is closer to the experimental solution in all the loading cases. Similar discrepancy of the Neuberger experimental results was also presented by Schwer [1]. The SPH-method also proved to be computationally more effective, which additionally highlights its advantages over the MM-ALE method. This is especially evident when larger scaled distances are involved.

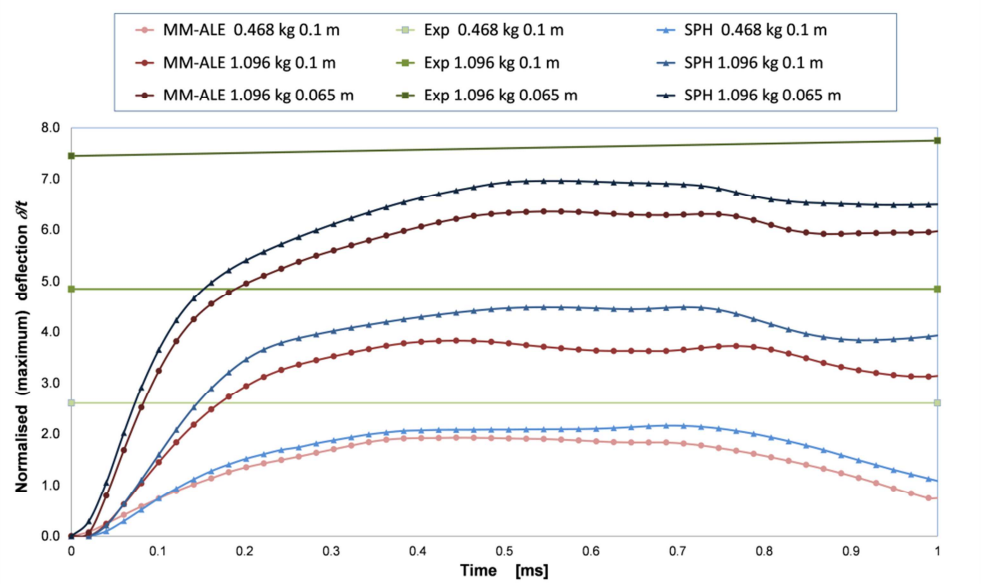


*Fig. 5: Time-deflection history: Flat plate results comparisons*

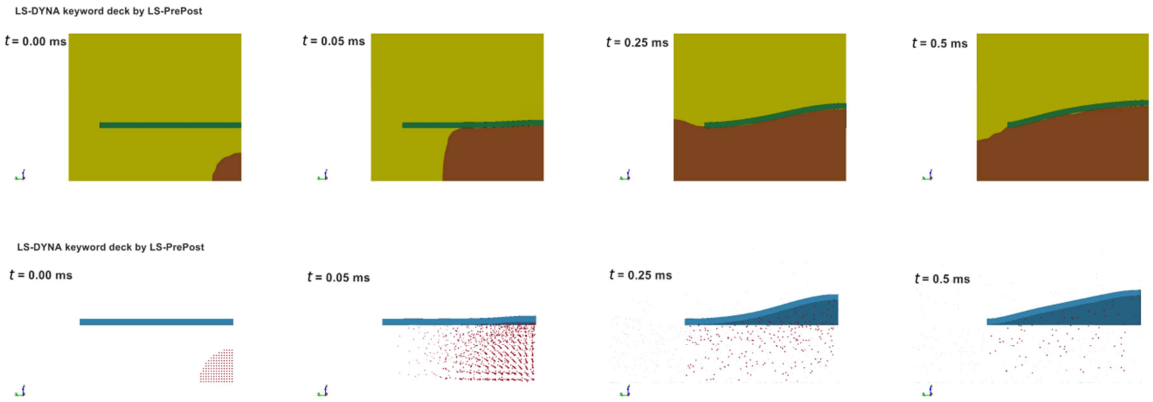


*Fig. 6: Flat plate models comparisons ($m_{TNT}$ = 1.094 kg, $h_{SoD}$ = 0.1 m)*

### 4.2 V-shaped plate

In the case of relatively small plate deflections when the mesh of the loaded plate/structure can still be considered parallel with the mesh of the ALE fluids, the "leakage" problem that may occur in MM-ALE model does not appear (Fig. 6). However, often irregular structure geometries should be analysed under blast loading effects caused by high explosives and the mesh parallelism cannot be always provided. For that purpose the results comparison using both models was performed analysing the blast response of a V-shaped plate. The same material models and material properties were used. The plate in both models was rotated for an angle of 45° around the longitudinal axes of symmetry in order to form a V-shaped plate with included angle of 90°. Time-displacement histories of the nodes placed at the plate centres for both models are presented in Fig. 7. It is evident that the maximum plate displacement of the MM-ALE model is 51% lower than the maximum plate displacement of the SPH model (Fig. 7), while blast loaded flat plate exhibit 12.5% displacement (Fig. 5).

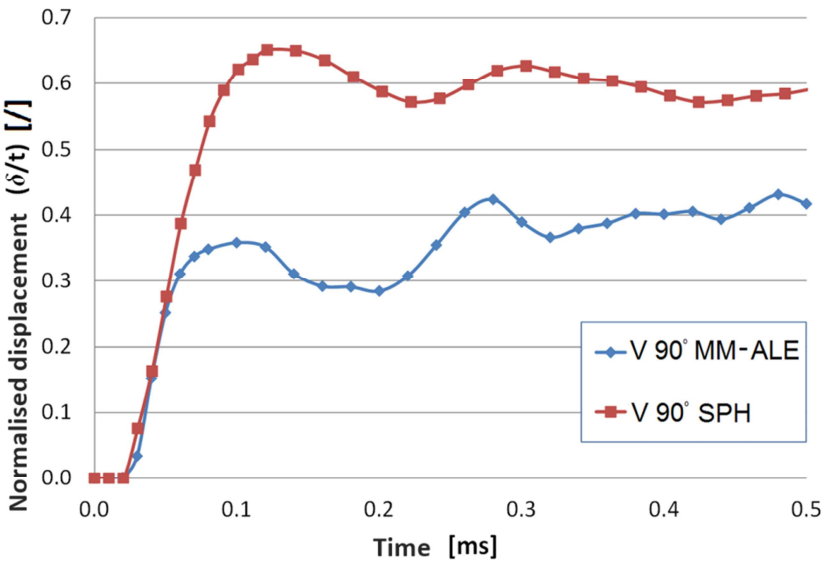


*Fig. 7: Time-deflection history: V-plate models comparison*

A more visual comparison of the plate response of both models is presented in Fig. 8 at four different time intervals. It is visible that “leakage” of the gas products on the other side of the plate is present with the MM-ALE model, without any appearance of a plate fracture. This causes a reduced energy transfer from the gaseous products to the plate and consequently the plate centre displacement is underestimated. On the other side, no visible “leakage” of SPH particles was observed in the SPH-model using the presented numerical parameters.

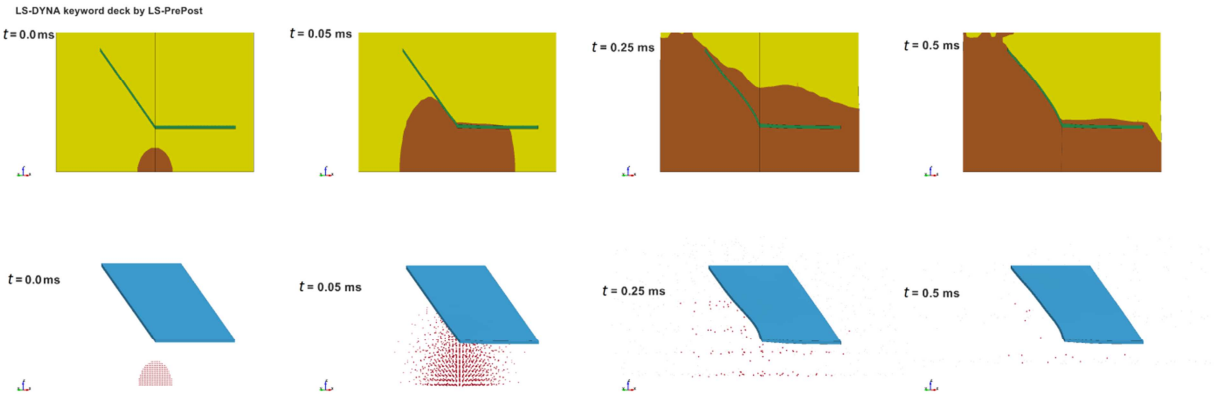


*Fig. 8: V-plate models comparison*

Fig. 9 presents three most often used mesh shapes (spherical and cube) for modelling blast wave development in space and its interaction with structural geometry. It is well known that spherical mesh (Fig. 9a) can yield the most precise approximation to the experimental results in each space direction, for blast wave development in free air, while the cube mesh (Fig. 9b, Fig. 9c) requires a much more refined mesh to achieve the same approximation of blast wave parameters in all space directions. However, in case of blast response analysis of most structural geometries the cube mesh appears to be much more practical for use.

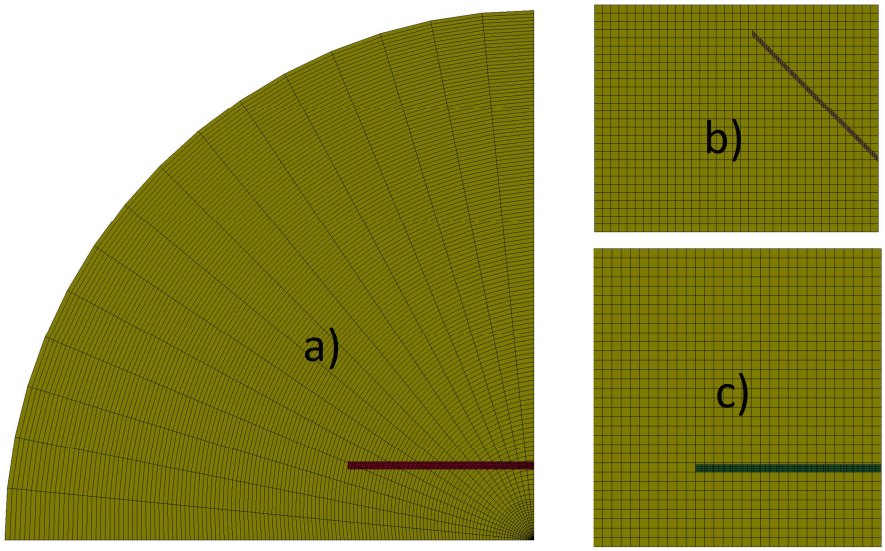


*Fig. 9: Time-deflection history: V-plate models comparison*

In the case of V-shaped plate, both fluid mesh shapes lack parallelism with the loaded plate (Fig. 9b) due to which fluids "leakage" can appear, consequently underestimating the structural plate deformation. To illustrate this, the three models presented in Fig. 9 were run and the plate response comparison is presented in Fig. 10 at four different time intervals. It is also visible that "leakage" of the gas products is present when fluids and structural meshes lack parallelism.

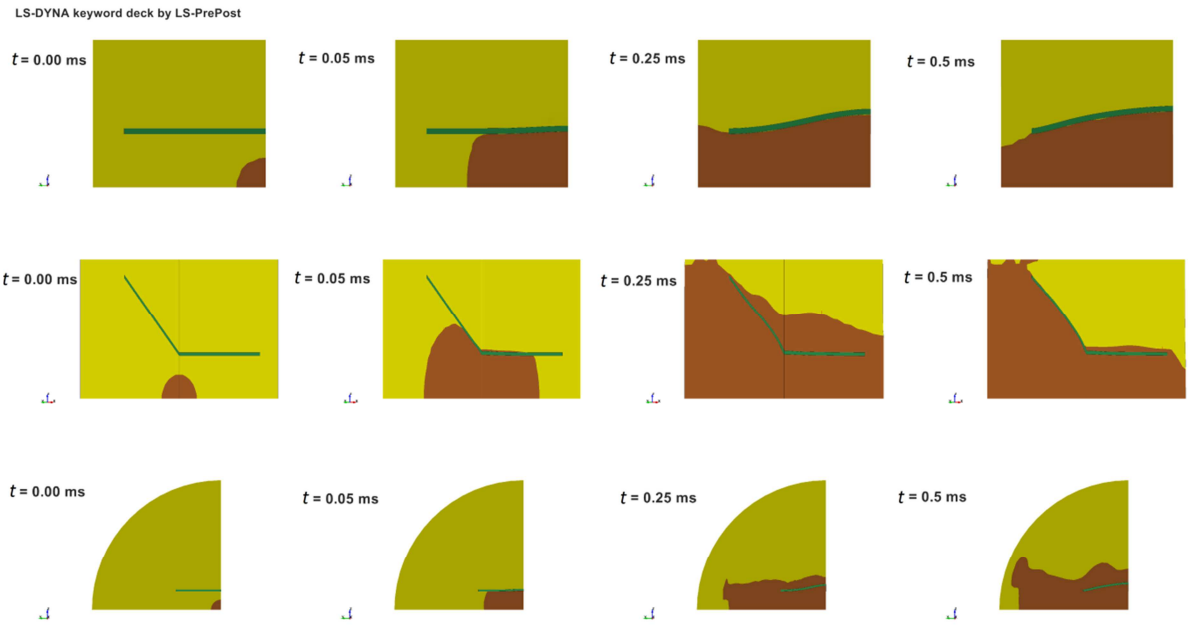


*Fig. 10: Appearance of leakage in the MM-ALE model*

## 5 Conclusions

In this paper, the MM-ALE and SPH modelling techniques were used for blast response analysis of flat and V-shaped plates. The results comparisons showed that the SPH modelling technique is

- **more precise**,
- **simpler to use** and
- **more computation- efficient** when compared to MM-ALE modelling technique.

The fluid "leakage" problem which is the main drawback of the MM-ALE modelling technique does not appear in SPH. Therefore, the SPH modelling technique is recommended to be used for blast response analysis of structures, at least for the scaled distances examined in this study ($Z$ = 0.063 m/kg$^{1/3}$ to $Z$ = 0.128 m/kg$^{1/3}$).

## 6 Literature

[1] Len Schwer, H. Teng, M. Souli, LS-DYNA Air Blast Techniques: Comparisons with Experiments for Close-in Charges, 10th European LS-DYNA Conference 2015, Würzburg, Germany, 2015.
[2] LSTC, LS-DYNA Keyword User's Manual, Volume I, Livermore, California, 2013.
[3] A. Alia, M. Souli, High explosive simulation using multi-material formulations, Applied Thermal Engineering 26(10) (2006) 1032-1042.
[4] M. Souli, A. Ouahsine, L. Lewin, ALE formulation for fluid–structure interaction problems, Computer Methods in Applied Mechanics and Engineering 190(5–7) (2000) 659-675.

[5] P.S. Todd, A coupling of empirical explosive blast loads to ALE air domains in LS-DYNA®, IOP Conference Series: Materials Science and Engineering 10(1) (2010) 012146.
[6] B. Luccioni, D. Ambrosini, R. Danesi, Blast load assessment using hydrocodes, Engineering Structures 28(12) (2006) 1736-1744.
[7] B. Zakrisson, B. Wikman, H.-Å. Häggblad, Numerical simulations of blast loads and structural deformation from near-field explosions in air, International Journal of Impact Engineering 38(7) (2011) 597-612.
[8] C.F. Zhao, J.Y. Chen, Y. Wang, S.J. Lu, Damage mechanism and response of reinforced concrete containment structure under internal blast loading, Theoretical and Applied Fracture Mechanics 61(0) (2012) 12-20.
[9] B. Zakrisson, H.-Á. Häggblad, P. Jonsén, Modelling and simulation of explosions in soil interacting with deformable structures, cent.eur.j.eng 2(4) (2012) 532-550.
[10] C. Soutis, G. Mohamed, A. Hodzic, Modelling the structural response of GLARE panels to blast load, Composite Structures 94(1) (2011) 267-276.
[11] M.S. Chafi, G. Karami, M. Ziejewski, Numerical analysis of blast-induced wave propagation using FSI and ALEmulti-material formulations, International Journal of Impact Engineering 36(10–11) (2009) 1269-1275.
[12] S. Chung Kim Yuen, G.S. Langdon, G.N. Nurick, E.G. Pickering, V.H. Balden, Response of V-shape plates to localised blast load: Experiments and numerical simulation, International Journal of Impact Engineering 46(0) (2012) 97-109.
[13] D.M. Fox, X. Huang, D. Jung, W.L. Fourney, U. Leiste, J.S. Lee, The response of small scale rigid targets to shallow buried explosive detonations, International Journal of Impact Engineering 38(11) (2011) 882-891.
[14] L.B. Jayasinghe, D.P. Thambiratnam, N. Perera, J.H.A.R. Jayasooriya, Computer simulation of underground blast response of pile in saturated soil, Computers & Structures 120(0) (2013) 86-95.
[15] G.S. Langdon, I.B. Rossiter, V.H. Balden, G.N. Nurick, Performance of mild steel perforated plates as a blast wave mitigation technique: Experimental and numerical investigation, International Journal of Impact Engineering 37(10) (2010) 1021-1036.
[16] X. Liu, X. Tian, T.J. Lu, D. Zhou, B. Liang, Blast resistance of sandwich-walled hollow cylinders with graded metallic foam cores, Composite Structures 94(8) (2012) 2485-2493.
[17] L. Ma, J. Xin, Y. Hu, J. Zheng, Ductile and brittle failure assessment of containment vessels subjected to internal blast loading, International Journal of Impact Engineering 52(0) (2013) 28-36.
[18] S.J. Pi, D.S. Cheng, H.L. Cheng, W.C. Li, C.W. Hung, Fluid–structure-interaction for a steel plate subjected to non-contact explosion, Theoretical and Applied Fracture Mechanics 59(1) (2012) 1-7.
[19] K. Spranghers, I. Vasilakos, D. Lecompte, H. Sol, J. Vantomme, Numerical simulation and experimental validation of the dynamic response of aluminum plates under free air explosions, International Journal of Impact Engineering 54(0) (2013) 83-95.
[20] Y.S. Tai, T.L. Chu, H.T. Hu, J.Y. Wu, Dynamic response of a reinforced concrete slab subjected to air blast load, Theoretical and Applied Fracture Mechanics 56(3) (2011) 140-147.
[21] J. Trajkovski, Odziv centralno in ekscentrično obremenjenih oklepnih pločevin " V " in " U " oblik pod vplivom eksplozijskega vala razstreliva, 2015.
[22] C. Antoci, M. Gallati, S. Sibilla, Numerical simulation of fluid–structure interaction by SPH, Computers & Structures 85(11–14) (2007) 879-890.
[23] M.A. Barsotti, J.M.H. Puryear, D.J. Stevens, R.M. Alberson, P. McMahon, Modeling Mine Blast with SPH, 12th International LS-DYNA User Conference, Detroit, USA, 2012.
[24] T. Genevieve, D. Robert, Finite element simulation using SPH particles as loading on typical Light Armoured Vehicles, 10th International LS-DYNA users conference, 2008.
[25] Geneviève Toussaint, Amal Bouamoul, Comparison of ALE and SPH methods for simulating mine blast effects on structures, DRDC Valcartier, Dec. 2010.
[26] J.-x. Xu, X.-l. Liu, Analysis of structural response under blast loads using the coupled SPH-FEM approach, J. Zhejiang Univ. Sci. A 9(9) (2008) 1184-1192.
[27] J. Trajkovski, R. Kunc, I. Prebil, Blast response of centrally and eccentrically loaded flat-, U-, and V-shaped armored plates: comparative study, Shock Waves (2016) 1-9.
[28] L. Olovsson, A.G. Hanssen, T. Børvik, M. Langseth, A particle-based approach to close-range blast loading, European Journal of Mechanics - A/Solids 29(1) (2010) 1-6.
[29] T. Børvik, L. Olovsson, A.G. Hanssen, K.P. Dharmasena, H. Hansson, H.N.G. Wadley, A discrete particle approach to simulate the combined effect of blast and sand impact loading of steel plates, Journal of the Mechanics and Physics of Solids 59(5) (2011) 940-958.
[30] Hailong Teng, J. Wang, Particle Blast Method (PBM) for the Simulation of Blast Loading, 13th International LS-DYNA Conference, Detroit, USA, 2014.

[31] D. Hilding, Methods for modelling Air blast on structures in LS-DYNA, Nordic LS-DYNA Users' Conference, Gothenburg, Sweden, 2016.
[32] A. Neuberger, S. Peles, D. Rittel, Scaling the response of circular plates subjected to large and close-range spherical explosions. Part I: Air-blast loading, International Journal of Impact Engineering 34(5) (2007) 859-873.
[33] J. Trajkovski, R. Kunc, J. Perenda, I. Prebil, Minimum mesh design criteria for blast wave development and structural response-MMALE method, Latin American Journal of Solids and Structures 11(11) (2014) 1999-2017.
[34] M.A.S. Len Schwer, James O'Daniel & Timothy M. Madsen, , Free air blast simulation: Engineering model and MM-ALE calculation.
[35] J.A. Zukas, W.P. Walters, Explosive Effects and Applications, Springer London, Limited2002.